Available online at www.sciencedirect.com
SCIENCE DIRECT
Composites: Part A 36 (2005) 1555–1561
composites Part A: applied science and manufacturing
www.elsevier.com/locate/compositesa

Thermo-mechanical properties of randomly oriented carbon/epoxy nanocomposites

J.D. Fidelus[a], E. Wiesel[a], F.H. Gojny[b], K. Schulte[b], H.D. Wagner[a,*]

[a]Department of Materials and Interfaces, Weizmann Institute of Science, 76100 Rehovot, Israel
[b]Polymer Composites, Technical University Hamburg-Harburg (TUHH), Denickestraße 15, D-21073 Hamburg, Germany

Received 14 October 2004; revised 17 February 2005; accepted 17 February 2005

Abstract

The thermo-mechanical properties of epoxy-based nanocomposites based on low weight fractions (from 0.01 to 0.5 wt%) of randomly oriented single- and multi-walled carbon nanotubes were examined. Preparation methods for the nanocomposites, using two types of epoxy resins, were developed and good dispersion was generally achieved. The mechanical properties examined were the tensile Young's modulus by Dynamic Mechanical Thermal Analysis and the toughness under tensile impact using notched specimens. Moderate Young's modulus improvements of nanocomposites were observed with respect to the pure matrix material. A particularly significant enhancement of the tensile impact toughness was obtained for specific nanocomposites, using only minute nanotube weight fractions. No significant change in the glass transition temperature of SWCNT/epoxy nanocomposites was observed, compared to that of the epoxy matrix. The elastic modulus of the SWNT-based nanocomposites was found to be slightly higher than the value predicted by the Krenchel model for short-fiber composites with random orientation.

Keywords: A. Nano-structures; B. Fracture toughness; B. Impact behavior; D. Mechanical testing; Carbon nanotubes

1. Introduction

The discovery of multi-walled carbon nanotubes (MWCNTs) [1] and single-walled carbon nanotubes (SWCNTs) [2] has generated new perspectives in many fields of science and technology [3,4]. Due to their structure (they consist of tiny concentric graphene cylinders), these novel forms of crystalline carbon possess an outstanding combination of electrical, thermal and mechanical properties [4–10]. Their extremely high strength to weight ratio [7], a very high Young's modulus in the TPa range [8,10], and high flexibility and toughness [10,11], make them a candidate material for future reinforced polymer matrix composites. Their mechanical properties (especially tensile strength) considerably exceed those of currently available fiber materials (graphite, Kevlar, stainless steel, …) [12]. To take full advantage of these unique mechanical properties, optimization of nanotube-polymer interface properties (such as wettability [13] and adhesion [14]) is required. For tensile stiffness and strength, wetting and adhesion (via chemical bonding between the nanotubes and polymer) are necessary for the efficient transfer of stress to the nanotubes [13–16], whereas for toughness, some slippage between nanotubes and the matrix (thus, relatively lower adhesion) might be desirable to capitalize on the flexibility and toughness characteristics of the nanotubes. Also, due to the high aspect ratio of carbon nanotubes (CNT), large interfacial areas are available for stress transfer. However, the large contact areas between carbon nanotubes and the relatively strong inter-tube attraction via van der Waal's forces (especially in SWCNTs [17]) create difficulties during their incorporation into polymers: the nanotubes spontaneously bundle together, which makes their dispersion more difficult, leading to a drastic decrease in the strength of nanocomposites. High-quality dispersion of nanotubes in polymer composites is, therefore, imperative for efficient structural reinforcement. Note also that small amounts of CNT spread into a polymer have been shown to affect the electrical properties (conductivity), and the thermal resistance, of nanotube-based composites [6,18].

* Corresponding author. Tel.: +972 8 342594; fax: +972 8 344137.
E-mail address: daniel.wagner@weizmann.ac.il (H.D. Wagner).

1359-835X/$ - see front matter © 2005 Elsevier Ltd. All rights reserved.
doi:10.1016/j.compositesa.2005.02.006

The focus of this work is to develop preparation methods to effectively disperse carbon nanotubes into an epoxy matrix, and to improve the mechanical properties of the resulting nanocomposites. We examine specific elastic and fracture properties of two types of epoxy resins in which two types of well-dispersed low weight fractions of carbon nanotubes were incorporated.

2. Materials and methods

2.1. Nanotubes and polymer matrices

The carbon nanotubes were (1) HiPCO SWCNTs (CNI Houston) with a length in the micron range and a diameter of 0.8–1.0 nm and (2) MWCNTs produced via chemical vapor deposition (CVD) (Nanolab), with nominal purity of 95%, length of 1–5 μm, external diameter of 30–40 nm and interlayer distance of 3.315 Å. For details, see [9]. Two types of epoxy resins were used: (1) LY 564 (Ciba-Geigy, Switzerland, hardener: HY 560) and (2) Epon 815 (Huntsman Corporation, Texas, hardener: Jeffamine^{R} T-403 polyetheramine). Both resins have low processing viscosity and good overall mechanical properties for composite applications.

2.2. Nanocomposite preparation

2.2.1. Preparation of pure resin specimens

LY 564 epoxy and HY560 hardener (weight ratio 100/27) were thoroughly mixed and put under vacuum for 35–40 min to remove air bubbles, then cast into a RTV mold and cured at 80 °C for 10 h. The Epon 815/T-403 specimens were prepared similarly (weight ratio 100/43), but with the following curing schedule: 2 h at 80 °C followed by 3 h at 125 °C.

2.2.2. Preparation of nanocomposites

A small amount (5–6 mg) of sodium dodecyl sulphate (SDS) surfactant was dissolved in about 1 mL of ethanol and two weight percentages (0.01 and 0.05) of SWCNTs were added to each of the solutions. Tetrahydrofuran (THF) was used for the preparation of suspensions of MWCNTs. Homogeneous suspensions were prepared using a high intensity sonicator (at 20% amplitude for 2 min) and a sonic bath (for 1 h). Each nanotube suspension was then added to an epoxy resin (2 g) and the components were mixed again using the high intensity sonicator (at 50% amplitude for 4 min). The mixtures were left overnight at 45 °C, followed by 1 h in vacuum, to evaporate the solvent. The hardener was then added (LY 564/HY 560 epoxy mixed in a 100:27 ratio, and Epon 815/T-403 epoxy mixed in a 100:43 ratio, respectively) and mechanically mixed with the epoxy/nanotube mixtures. These mixtures were returned to vacuum for 35–40 min (for LY564/HY560) or 90–100 min (for Epon 815/T-403), respectively, to remove any air trapped during mixing, and to ensure homogeneity. The mixtures were then cast into a rectangular RTV mold (50 mm$\times$5 mm$\times$0.8 mm^3) and cured at 80 °C for 10 h (for LY564/HY560) or left at room temperature for 24 h and then cured at 80 °C for 2 h and 125 °C for 3 h (for Epon 815/T-403). These methods produced non-porous composites with good nanotube dispersion, as observed using high resolution scanning electron microscopy (Philips XL30, The Netherlands). A thin layer (about 3 nm) of chromium was sputter-coated on the SEM specimens, which were mounted onto a standard SEM holder with conducting carbon tape.

2.3. Dynamic mechanical thermal analysis (DMTA)

Tensile DMTA tests were performed to generate thermomechanical data for the nanocomposites. An 'EPLEXOR 500 N' apparatus (GABO, Germany) was employed for those tests, using 50$\times$5$\times$0.8 mm^3 specimens. The samples were tested in the 0–130 °C temperature range, at a heating rate of 3 °C/min in air and at a frequency of 10 Hz. The storage modulus (E'), complex modulus (E^*) and the loss tangent (tan δ) were determined as a function of temperature. Three specimens were tested for each type of material (LY564 and Epon 815 and their nanocomposites). The specimen-to-specimen variation of the storage modulus was generally very small (of the order of $\pm$0.38% for LY564 and of $\pm$1.3% for Epon 815).

2.4. Impact tests

Impact tests were performed in tension with double-notched specimens, using a Zwick Impact Testing apparatus. The specimen thickness was 0.22 mm, the width 3 mm, and the gauge length used was 20 mm (total specimen length was 30 mm). Two 0.4 mm deep V-shaped notches were machined on both sides of the specimen width. A 0.5 J pendulum and test piece yoke of 15 g were used for impact.

3. Results and discussion

3.1. SWCNT/epoxy nanocomposites

SWCNTs agglomerates of ropes (diameter of about 12 nm) are present and uniformly dispersed into the LY 564 epoxy specimens, as observed by optical and high resolution scanning electron microscopy observations. The same is true for the Epon 815 epoxy specimens although the dispersion of the agglomerates was somewhat less uniform. The storage modulus and tan δ are presented in Fig. 1 as a function of temperature and of CNT content (0.01 and 0.05 wt%), for both epoxies. Below 50 °C the storage modulus of the LY 564-based composites increases by a few percent relative to the pure epoxy (Fig. 1(a)). In parallel, a decrease of the tan δ peak height is observed with increasing

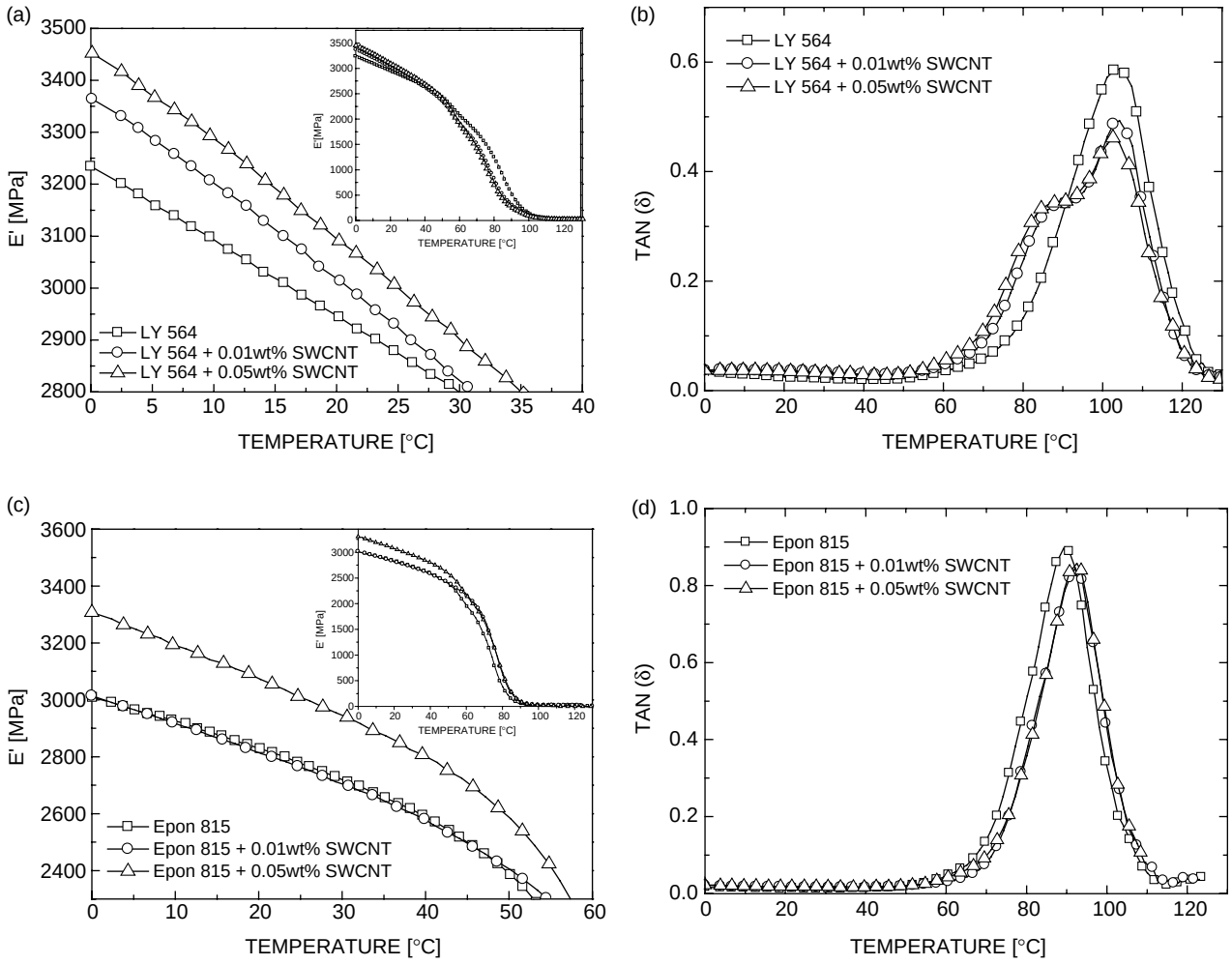

Fig. 1. (a) Storage modulus (E') as a function of temperature (T) for LY 564 with and without SWCNTs, (b) Loss tan δ as a function of temperature for LY 564 with and without SWCNTs, (c) Storage modulus (E') as a function of temperature (T) for Epon 815 with and without SWCNTs, (d) Loss tan δ as a function of temperature for Epon 815 with and without SWCNTs.

nanotube content (Fig. 1(b)). A similar picture emerges for the Epon 815 composites (Fig. 1(c and d)), although the absolute values of tan δ are higher for Epon 815 (about 0.9) than for LY 564 (about 0.6), and the decrease in peak height maximum for the Epon 815 nanocomposites is proportionally smaller than for the LY 564 nanocomposites. To clarify these results, a plot of the normalized modulus at room temperature against CNT content is presented in Fig. 2 for both types of composites. A comparison is made with a Rule-of-Mixture (RoM) type prediction of the modulus E (based on Krenchel's model for 3-dimensional randomly dispersed short-fiber composites [19,21]):

$$E_C = \eta E_{NT} V_{NT} + E_m(1 - V_{NT}) \quad (1)$$

where V is the volume fraction (the subscripts C, NT and m denote composite, nanotube and matrix, respectively), and η is Krenchel's coefficient which, for 3D randomly oriented rods, is 0.2 [19,20]. For convenience, the assumed nanotube modulus used in Eq. (1) was 1 TPa for both tube types.

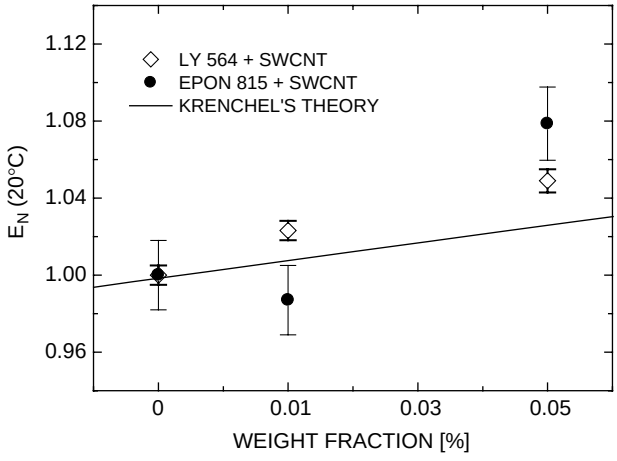

Fig. 2. A comparison between the experimental (DMTA) data for the normalized Young's modulus ($E_N = E_{Composite}/E_{Resin}$) and the model of Krenchel. The complex moduli at 20 °C of LY 564 epoxy and Epon 815 epoxy are 2945 and 2828 MPa, respectively.

Note also that to satisfy the model's assumptions, it is loosely assumed that all nanotubes are straight, have the same length, and that perfect interfacial bonding exist as required by Krenchel's model as well. The volume fraction (V_{NT}) of carbon nanotubes was calculated from the mass fraction of nanotubes, m_{NT}, assuming two phases and no trapped air, using

$$V_f = \left[\frac{\rho_r}{m_{NT}} - \rho_r + 1\right]^{-1} \quad (2)$$

where $\rho_r = \rho_{NT}/\rho_m$ is the ratio of nanotube to matrix density. We used $\rho_{NT} = 1.4$ g/cm^3 for SWCNTs [9] and 1.72 g/cm^3 for MWCNTs (average value from calculations, see Eq. (14) in Ref. [21]) respectively, and 1.2 and 1.1 g/cm^3 for the LY 564 and Epon 815 matrices, respectively. The experimental modulus (at 20 °C) of SWCNT/LY564 nanocomposites increases slightly faster with CNT content than predicted by the RoM. It is also seen that, for 0.05 wt% SWCNT/Epon 815 nanocomposites, an 8% modulus increase is measured relative to the polymer. Such modulus increases at very low nanotube loadings suggest that the load is transferred efficiently from the matrix to the SWCNTs, with the obvious implications regarding interfacial adhesion. Note that only slight variations in T_g were observed for both types of SWCNT-based nanocomposites, as a function of tube content, see Fig. 3.

A substantial increase in tensile impact strength was measured (Fig. 4), relative to the pure matrices. The improvement ranges between 18 and 35%, respectively, for both resins, within the 0.01–0.05 wt fraction span. High resolution SEM micrographs of pure epoxy and of SWNT/epoxy composites after impact did not reveal anything unforeseen, namely, pure epoxy fracture surfaces were glassy-like whereas the nanocomposite fracture surfaces were rougher in appearance (more so for SWCNT/LY564 than for SWCNT/Epon815). The increase in impact strength (and thus, possibly, of toughness) may be explained by

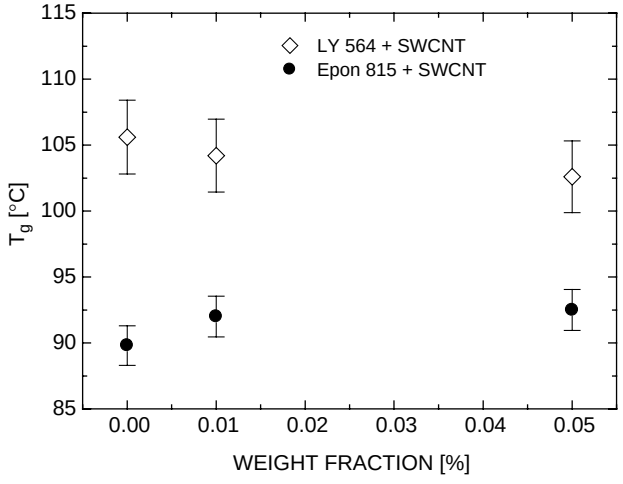

Fig. 3. Glass transition temperature as a function of SWCNTs weight content for LY 564 and Epon 815.

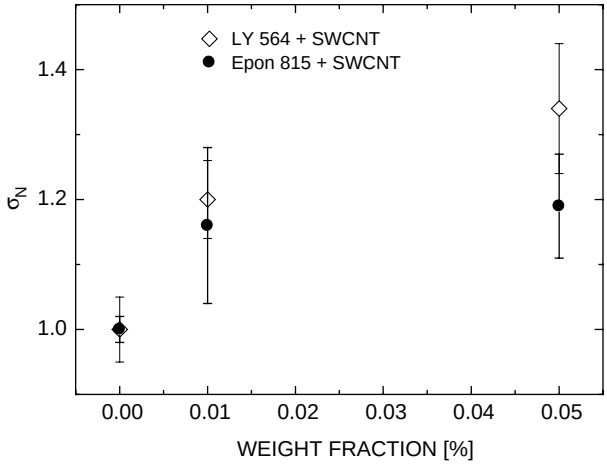

Fig. 4. Normalized tensile impact strength ($\sigma_N = \sigma_{Composite}/\sigma_{Resin}$) as a function of SWCNT weight fraction. The impact strength of LY 564 epoxy is 122.9 kJ/m^2, and that of Epon 815 is 161.7 kJ/m^2.

the presence of cavities bridged by nanotube ropes (mainly in the SWCNT/LY564 composites), which leads to energy dissipation by nanotube pull-out. Note also that such ropes are observed (using high resolution SEM) to be well wetted by epoxy, as in our earlier TEM work using SWCNT/LY564 films [14,22]. An additional contribution to energy dissipation arises from the crack deflection at agglomerates.

3.2. MWCNT/epoxy nanocomposites

The quality of the dispersion of MWCNTs in epoxy was similar to that of SWCNTs in epoxy, with again the dispersion in Epon 815 being slightly less uniform than in LY564. Also, the variation of the storage modulus of both types of MWCNT-based composites (Fig. 5) with increasing tube content, is generally the same as for SWCNT-based composites. A plot of the normalized (room temperature) modulus against nanotube content is presented in Fig. 6, for both types of epoxy-based composites. The complex composite modulus lies above the matrix modulus at all nanotube contents. As before, the modulus at 0.05 wt% MWCNT is higher than the Rule of Mixtures prediction. However, at 0.5 wt% MWCNTs, the modulus is lower than the RoM prediction, perhaps due to less than ideal properties of the MWCNTs and to the possible relative slippage (telescopic behavior) of the shells in multi-walled nanotubes [14,16,22], which would lead to poor load transfer in tension [14]. Finally, as before with SWCNT systems, the absolute values of tan δ (about 0.9) are higher for the Epon 815 system than for the LY 564 system (about 0.6).

A significant reduction in glass transition temperature is observed in the tan δ plots for 0.5 wt% MWCNT/LY564 nanocomposites. This is made more evident by plotting T_g against tube content, in Fig. 7. By contrast, the Epon 815 system shows no change in T_g.

The tensile impact strength results are presented in Fig. 8. As with SWCNT systems, a substantial impact resistance

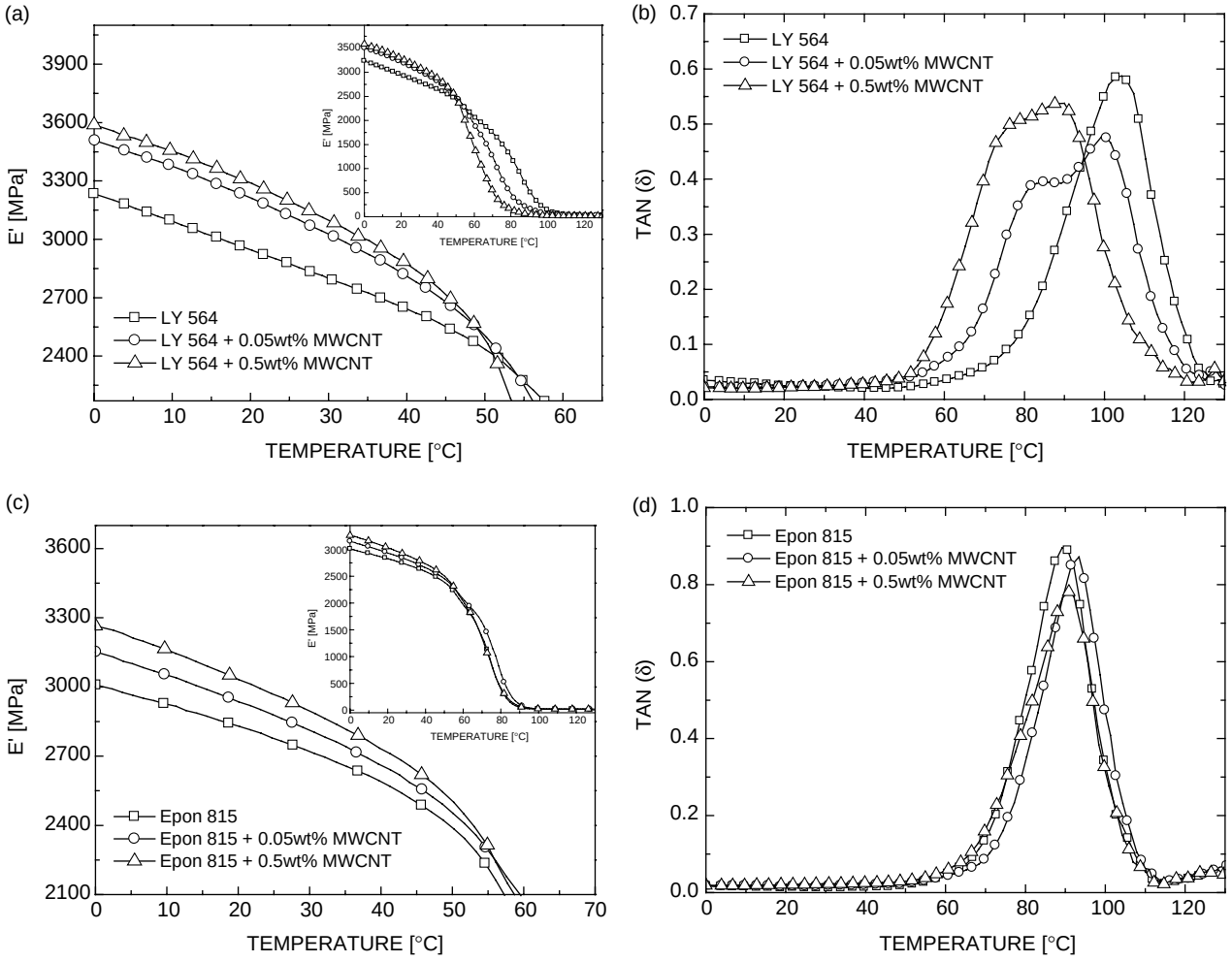

Fig. 5. (a) Storage modulus (E') as a function of temperature (T) for LY 564 with and without MWCNTs, (b) Loss tan δ as a function of temperature for LY 564 with and without MWCNTs, (c) Storage modulus (E') as a function of temperature (T) for Epon 815 with and without MWCNTs, (d) Loss tan δ as a function of T for Epon 815 with and without MWCNTs.

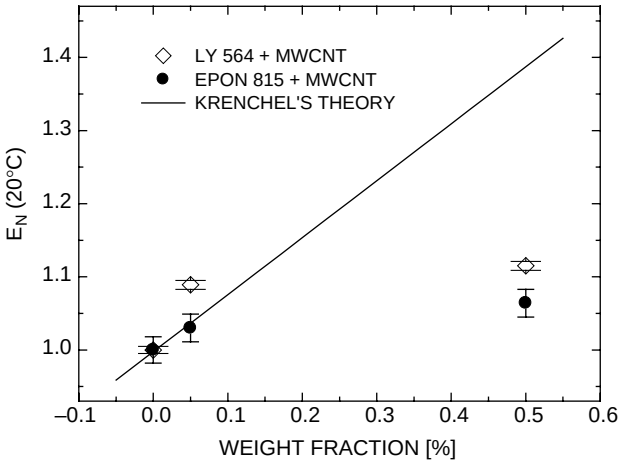

Fig. 6. Comparison between normalized Young's modulus ($E_N = E_{Composite}/E_{Resin}$) using Krenchel's model and from DMTA investigations.

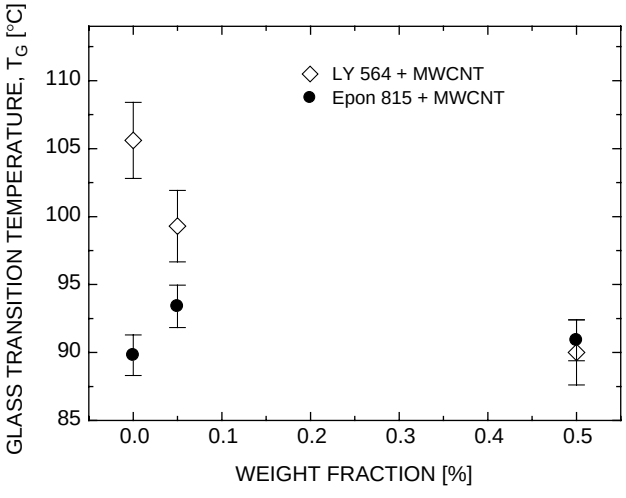

Fig. 7. Glass transition temperature as a function of MWCNTs weight percentage for LY 564 and Epon 815.

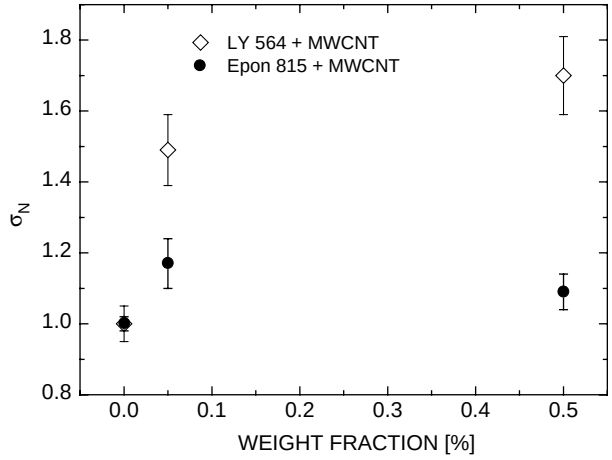

Fig. 8. Normalized tensile impact strength ($\sigma_N = \sigma_{Composite}/\sigma_{Resin}$) as a function of weight fraction of MWCNTs.

arises with respect to the pure matrices for the LY 564 system: up to 70% when using 0.5 wt% MWCNTs, and up to 50% when using 0.05% MWCNTs. The Epon 815 system is much less impact-performant. As with SWCNTs composites, nanocomposite fracture surfaces generally appear to be rather rough in the SEM, more so for MWCNT/LY564 than for MWCNT/Epon815. Enhanced toughness in the LY 564 system is explained as before by the good dispersion clearly seen in the SEM (Fig. 9) and the good wetting of the tubes by the matrix. Note that the possibility of enhanced toughness of samples due to residual SDS surfactant and solvent was readily rejected. Indeed, separate measurements using pure resin, and pure resin with solvents/surfactants similar to the specimens containing nanotubes, were also prepared and tested. Their static mechanical properties (such as Young's modulus) showed no change compared to the neat resin. If solvent/surfactant had remained in the system, a decrease of Young's modulus or tensile strength would certainly have been observed,

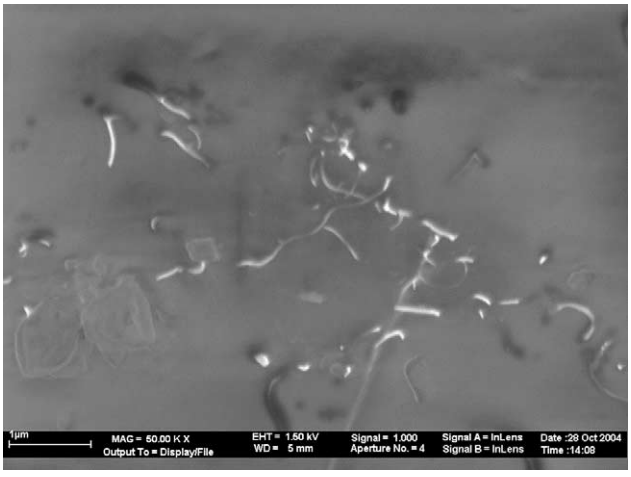

Fig. 9. SEM micrograph of the fracture surface of MWCNT/LY564 nanocomposites (0.5% bw), showing good nanotube dispersion.

which was not the case. Note also that the amount of SDS surfactant in the matrix system was only about 0.2 wt%.

It is interesting to notice that for the LY564 systems (with both SWCNT and MWCNT) the glass transition temperature decreases as more nanotubes are present (Figs. 3 and 7), most likely because these reduce the crosslinking tendency of the resin. This is also reflected by the shoulder in the tan(δ) that appears when nanotubes are added (Figs. 1(b) and 5(b)), and can be correlated with the impact strength increase as well (Figs. 4 and 8). Very little of this is seen with the Epon system, however.

We might ask—a posteriori—whether the aspect ratio L/D_{NT} (L is the tube length, D_{NT} is its external diameter) of carbon nanotubes (both SWNT and MWNT) is, in fact, large enough to allow sufficient stress transfer and, thus, to permit full exploitation of the nanotubes mechanical potential. The experimentally observed aspect ratios of SWCNTs and MWCNTs are, respectively, 500–1400 and 50–500. According to a simple model [23], the nanotubes are able to reach their maximum tensile strength under tension when the aspect ratio is at least equal to

$$\frac{L}{D_{NT}} = \frac{\sigma_{NT}}{2\tau_{NT}}\left(1 - \frac{d_{NT}^2}{D_{NT}^2}\right)$$

where σ_{NT} is the maximum strength of the tube, τ_{NT} is the interfacial shear strength between the nanotube and the polymer matrix, and d_{NT} is the internal diameter of the tube. For SWCNTs, using the conservative estimates $\sigma_{NT} =$ 50 GPa [24,25] and $\tau_{NT} = 35$–200 MPa [25,26], $d_{NT} =$ 0.81 nm, and $D_{NT} = d_{NT} + 0.68$ nm, the aspect ratio range calculated from the expression above is 120–700. Similarly, for MWCNTs, using a tube length of 1–5 μm, an external diameter of 30–40 nm, and an assumed internal diameter of 20 nm, the aspect ratio range calculated from the expression above is 70–625. Thus for both SWCNTs and MWCNTs, the experimentally observed aspect ratios are sufficiently large (compared to the range of calculated values) to enable efficient stress transfer. Finally, note that fracture toughness increases have also been recently observed in double-walled carbon nanotube-based composites [27].

4. Conclusions

The dynamic mechanical behavior and tensile impact properties of epoxy-based nanocomposites containing low weight fractions of MWCNTs and SWCNTs were studied. Satisfactory nanotube dispersion was achieved for both types of nanotubes into epoxy resins in the 0.01–0.5 wt% range. Improvements in complex modulus were obtained relative to the polymer matrix. Generally better damping properties are observed for Epon 815 and its composites compared with LY564 and its composites. A particularly significant improvement (70% reinforcement) in tensile impact strength was obtained for the 0.5 wt% MWCNT/LY564 system.

A simple calculation shows that the range of aspect ratios used here for both SWCNT and MWCNT enables efficient stress transfer, and thus permits the full exploitation of the nanotubes mechanical potential.

Acknowledgements

This project was supported by the (CNT) Thematic European network on 'Carbon Nanotubes for Future Industrial Composites' (EU), the Minerva Foundation, the G.M.J. Schmidt Minerva Centre of Supramolecular Architectures, and by the Israeli Science Foundation (Grant No 290/02). Thanks are due to Dr Asa Barber for help with the electron microscope work. H.D. Wagner is the incumbent of the Livio Norzi Professorial Chair, and wishes to acknowledge the inspiring aid of L. Hampton.

References

[1] Iijima S. Nature 1991;354:56. As a matter of fact, carbon-based nanotubes were discovered several years earlier by Nesterenko et al. Their work remains largely unknown to the scientific community [A.M. Nesterenko, N.F. Kolesnik, Y.S. Akhmatov, V.I. Sukhomlin, O.V. Prilutski, Metals 3 (1982), UDK 869.173.23, News of the Academy of Science, USSR, 12–16].
[2] Iijima S. Nature 1993;363:603. Bethune DS, Kiang CH, Devries MS, Gorman G, Savoy R, Vazquez J, et al. Nature 1993;363:605.
[3] Ajayan PM, Iijima S. Nature 1993;361:333.
[4] Thostenson ET, Ren ZF, Chou T-W. Compos Sci Technol 2001; 61:1899.
[5] Wildoer JWG, Venema LC, Rinzler AG, Smalley RE, Dekker C. Nature 1998;391:59. Odom TW, Huang J-L, Kim P, Lieber CM. Nature 1998;391:62.
[6] Hone J, Batlogg B, Johnson AT, Fischer JE. Science 2000;298:1730.
[7] Ruoff RS, Lorents DC. Carbon 1995;33:925.
[8] Treacy MMJ, Ebbesen TW, Gibson JM. Nature 1996;381:678.
[9] The information concerning CNTs can be found in the following web sites: SWCNTs (http://www.cnanotech.com), MWCNTs (http://www.nano-lab.com/powders.html).
[10] Wong EW, Sheehan PE, Lieber CM. Science 1997;277:1971.
[11] Falvo MR, Clary GJ, Taylor RM, Superfine R, Chi V, Brooks FP, et al. Nature 1997;389:582.
[12] Lau K-T, Hui D. Compos: Part B 2002;33:263.
[13] Barber AH, Cohen S, Wagner HD. Phys Rev Lett 2004;92(18): 1861031.
[14] Lourie O, Wagner HD. Appl Phys Lett 1998;73:3527.
[15] Wagner HD, Lourie O, Feldman Y, Tenne R. Appl Phys Lett 1998; 72:188.
[16] Schadler LS, Giannaris SC, Ajayan PM. Appl Phys Lett 1998;73: 3842.
[17] Girfalco AL, Hodak M, Lee SR. Phys Rev B 2000;62:13104.
[18] Sandler J, Shaffer MSP, Prasse T, Bauhofer W, Schulte K, Windle AH. Polymer 1999;40:5967.
[19] Krenchel, H. Fibre Reinforcement, Akademisk Forlag, Copenhagen; 1964.
[20] Fukuda H. Fibre Sci Technol 1974;7:207.
[21] Thostenson ET, Chou T-W. J Phys D: Appl Phys 2003;36:573.
[22] Gojny FH, Nastalczyk J, RosŁaniec Z, Schulte K. Chem Phys Lett 2003;370:820.
[23] Wagner HD. Chem Phys Lett 2002;361:57.
[24] Yu MF, Lurie O, Dyer MJ, Moloni K, Kelly TF, Ruoff RS. Science 2000;287:637.
[25] Cooper CA, Cohen SR, Barber AH, Wagner HD. Appl Phys Lett 2002;81:3873.
[26] Barber AH, Cohen S, Wagner HD. Appl Phys Lett 2003;82(23):4140.
[27] Gojny FH, Wichmann MHG, Köpke U, Fiedler B, Schulte K. Compos Sci Technol 2004;64:2363.